International Journal of Nanomedicine

Dovepress
open access to scientific and medical research

Open Access Full Text Article

ORIGINAL RESEARCH

Pyridine azo disperse dye derivatives and their selenium nanoparticles (SeNPs): synthesis, fastness properties, and antimicrobial evaluations

This article was published in the following Dove Press journal:
International Journal of Nanomedicine

International Journal of Nanomedicine downloaded from https://www.dovepress.com/
For personal use only.

Huda SA Alnassar[1]
Maher HE Helal[2]
Ahmed A Askar[3]
Doaa M Masoud[2]
Amira EM Abdallah[2]

[1]Department of Laboratories Technology, College of Technological Studies, Public Authority for Applied Education and Training, Fayha 70654, Kuwait; [2]Department of Chemistry, Faculty of Science, Helwan University, Cairo 11795, Egypt; [3]Departments of Botany and Microbiology, Faculty of Science (Boys), Al-Azhar University, Cairo 11751, Egypt

Aim: Aiming to produce pyridine azo disperse dyes with good fastness properties and promising antimicrobial activity, a number of novel systems of polyfunctionalized pyridine azo dyes and their selenium nanoparticles (SeNPs) were synthesized.

Materials and methods: The synthesized products were formed by the reaction of diazotized aniline derivatives or diazotized amino antipyrene with any of dibenzoyl methane or benzoyl acetone and cyanoacetamide in boiling ethanolic sodium ethoxide. The structures of the newly synthesized compounds were elucidated by elemental analysis and spectral data. Moreover, (SeNPs) of the pyridine azo disperse dyes were characterized by Ultra-Violet -Visible spectrophotometry, dynamic light scattering , X-ray diffraction, and transmission electron microscope analysis. On the other hand, the synthesized dyes and its (SeNPs) were applied for disperse dyeing of nylon 66 and their fastness properties were measured, such as washing, rubbing, perspiration, and light fastness. In addition, the antimicrobial activities for all the synthesized compounds and for (SeNPs) prepared compounds (**2bN, 2cN, 2fN, 2gN, 2hN**) were evaluated.

Results: Compounds **2bN, 2c, 2cN, 2fN, 2gN, 2h, 2hN**, and **2i** were the most active compounds against all Gram-positive and Gram-negative bacterial species. While, compounds **2b, 2f, 2g**, and **5b** were the most active toward some of the bacterial strains (at least two from the selected four strains). Moreover, compounds **2bN, 2cN, 2fN, 2gN, 2h, 2hN** showed higher activity toward the fungal strain. Also, the minimal inhibitory concentrations for all the most active compounds were determined.

Conclusion: Finally, all the (SeNPs) compounds revealed higher activity against bacterial and fungal strains than the other synthesized compounds.

Keywords: pyridine azo dyes, (SeNPs) azo dye, fastness properties, dyeing, antimicrobial, minimal inhibitory concentrations (MIC)

Introduction

Pyridine ring containing azo dyes has many advantages, including a color deepening effect as an intrinsic property of the pyridine ring and small molecular structure leading to better dye ability. The heterocyclic nature of the pyridine ring has also allowed for excellent sublimation fastness on the dyed fibers.[1] A number of researchers have studied aminopyridine derivatives as azo disperse dyes in the dyeing of synthetic fibers[2–5] and blended polyester/wool fibers. Pyridinone disperse dye derivatives have found many applications on several fibers due to their improved light fastness and brightness.[6–10] The novel compounds could lead to

Correspondence: Amira EM Abdallah
Department of Chemistry, Faculty of Science, Helwan University, Ain Helwan, Cairo 11795, Egypt
Tel +20 109 176 9838
Email amiraelsayed135@yahoo.com

submit your manuscript | www.dovepress.com
DovePress
http://doi.org/10.2147/IJN.S216914

© 2019 Alnassar et al. This work is published and licensed by Dove Medical Press Limited. The full terms of this license are available at https://www.dovepress.com/terms.php and incorporate the Creative Commons Attribution – Non Commercial (unported, v3.0) License (http://creativecommons.org/licenses/by-nc/3.0/). By accessing the work you hereby accept the Terms. Non-commercial uses of the work are permitted without any further permission from Dove Medical Press Limited, provided the work is properly attributed. For permission for commercial use of this work, please see paragraphs 4.2 and 5 of our Terms (https://www.dovepress.com/terms.php).

the development of new functional materials with special finish properties for textile fabrics. Moreover, pyridinone ring system having very interest as biologically active compound especially as antimicrobial,[11–15] anticancer,[16] antiviral,[17] anti-inflammatory, and analgesic[18] antioxidant agents.[19] On the other hand, nanoparticles hold promise as innovative materials with new electronic, magnetic, and catalytic properties.[20–25] Several of nanostructures, involving metal nanoparticles (Ag, Ce, Au, Eu, Cu, Fe, Se, Ti, Zn, etc.), polymers, carbon and silicon-based nanomaterials have been utilized as effective drug delivery carriers and therapeutic agents.[26–33] In the field of nanotechnology, some of metal nanoparticles such as Ag, Au, Ce, Fe, Se, Si, Ti, and Zn have a special position as they display a unique scope not only as theranostic agents but possess large potential as carriers for chemotherapeutic agents, proteins, etc. Among these nanoparticles, selenium nanoparticles (SeNPs) are one of the most extensively studied due to their effective physical and chemical properties.[34] It has been found that many metal or metal oxide nanoparticles have many important applications as biologically active systems especially as antimicrobial agents.[35–42] We report herein as continuation to our interest in the design of bioactive heterocyclic compounds,[43–48] the preparation of novel dihydropyridinone disperse azo dyes derivatives with their SeNPs and their application as disperse dyes for the dyeing of nylon 66. The fastness properties and the antimicrobial activities of these dyes were also studied.

Materials and methods

Materials

All melting points were uncorrected and determined on an electrothermal apparatus (Büchi 535, Switzerland) in an open capillary tube. IR spectra were recorded on Fourier transform infrared spectrometer (FT-IR) JASCO FT-IR-3600 infrared spectrometer by employing KBr Pellet technique. UV-visible spectra were recorded on UV-visible spectrophotometer (UV-Vis.) JASCO V-560. ^{1}H-NMR and ^{13}C-NMR spectra were recorded on a Mercury-300BB (400 and 100 MHz, respectively), at Cairo University, in DMSO-*d6* as solvent using TMS [Si $(CH_3)_4$] as internal standard and chemical shifts are expressed as δ ppm. Mass spectra were recorded using Shimadzu (Japan) GC-MS-QP5050 prop Thermo Scientific. Elemental analyses were carried out on Vario EL III Elemental CHNS analyzer (Japan). Average particle size and size distribution were determined by dynamic light scattering (DLS) PSS-NICOMP 380-ZLS particle sizing system St. Barbara, California, USA. The size and morphology of the synthesized nanoparticles were recorded by using transmission electronmicroscope (TEM) model JEOL electron microscopy JEM-100 CX. X-ray diffraction (XRD) was recorded by Shimadzu apparatus using nickel-filter and Cu-Ka target, Shimadzu Scientific Instruments (SSI), Kyoto, Japan. Antibacterial and antifungal activities were performed at the bacteriology laboratory, Botany and Microbiology department, Faculty of Science, Al-Azhar University, Cairo, Egypt. Color strength (K/S) of the dyed samples was measured by using OPTIMATCH 3100. The colorfastness to washing was determined using Launder-ometer. Colorfastness to rubbing was determined using Crock-Meter Type FD II and colorfastness to perspiration was determined using Perspiration Tester. The light fastness test was measured by using Xenon Arc lamp. The tested fabric used throughout this work; namely nylon 66 was supplied by Misr-Helwan Company for spinning and weaving, Helwan, Cairo, Egypt. All the fastness properties test done by National Institute for Standards, Cairo, Egypt. Selenious acid was purchased from Sigma-Aldrich Company. The bacterial strains were obtained from American Type Culture Collection (ATCC), while the fungal strain was obtained from Regional Center of Mycology and Biotechnology (RCMB). Synthetic pathways are presented in Figures 1 and 2. Fastness properties, antimicrobial evaluations, and minimal inhibitory concentrations (MIC) of the newly synthesized products were expressed through Tables 1–3 and through Figures 9–12.

Synthetic procedures

General procedure for the preparation of 2-oxo-6-phenyl-5-(phenyldiazenyl)-1,2-dihydropyridine-3-carbonitrile derivatives (2a-j) and 5-((1,5-dimethyl-3-oxo-2-phenyl-2,3-dihydro-1h-pyrazol-4-yl)diazenyl)-2-oxo-6-phenyl-1,2-dihydropyridine-3-carbonitrile derivatives (5a,b)

To a cold solution (0–5°C), of any of 4-chloroaniline (1.27 g, 0.01 mol), 4-bromoaniline, (1.72 g, 0.01 mol), 4-nitroaniline (1.38 g, 0.01 mol), dichloroaniline (1.62 g, 0.01 mol), dimethoxyaniline (1.53 g, 0.01 mol) or aminoantipyrene (2.03 g, 0.01 mol), in hydrochloric acid (0.03 mol), sodium nitrite solution (0.69 g, 0.01 mol) were added drop by drop. To the later solution, a mixture of any of benzoyl acetone (1.62 g, 0.01 mol) or dibenzoyl

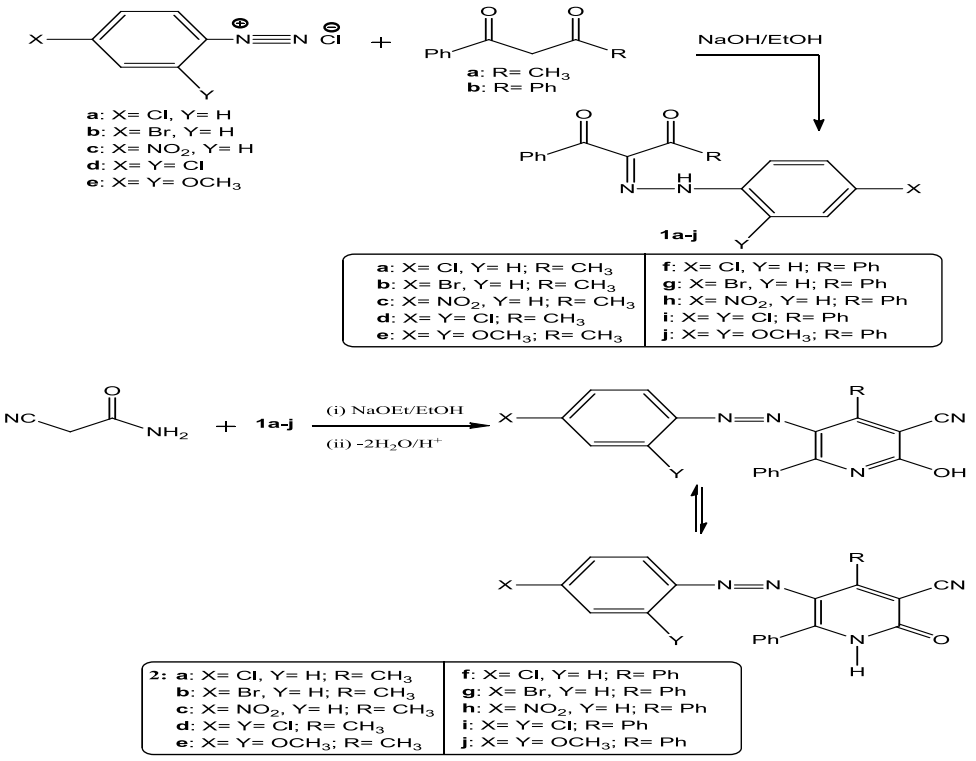

Figure 1 Synthesis of phenyldiazenyl pyridine derivatives (**2a–j**).

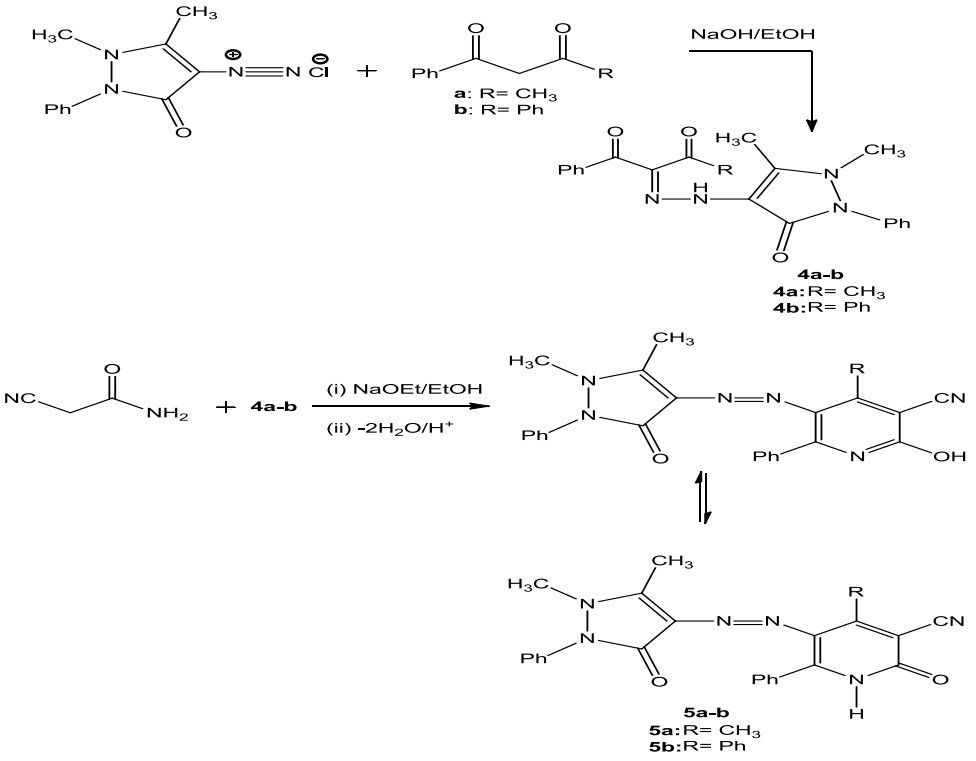

Figure 2 Synthesis of pyrazolyl diazenyl pyridine derivatives (**5a–b**).

Table 1 Fastness properties of azo disperse dyes on nylon 66

Dye	K/S[a] at λ_{max}=400 nm	Fastness to rubbing		Washing fastness at 90°C	Fastness to perspiration				Light
					Acidic		Alkaline		
		Dry	Wet	Alteration	Alteration	Staining	Alteration	Staining	
2b	3.28	1	2	1	4	3/4	4	3/4	4
2bN	3.20	4/5	4	2	3	3/4	3/4	3/4	2
2c	2.72	2	1	2	4	4	4/5	5	4
2cN	2.80	3	2	2	3	5	4	2	4
2f	2.98	2	3	3/4	3	2	4	2	3/4
2fN	2.79	3	3/4	3	3	4	2/3	4	3/4
2g	3.08	1	1	4/5	4	4	4	4	4
2gN	2.91	4/5	4/5	3/4	4	4	4	3	3/4
2h	3.48	2	1	3/4	3	4	4	2	4
2hN	3.54	4/5	4	1	2/3	4	3/4	2	2/3

Note: [a]K/S = (1−R)2/2R.
Abbreviations: R, a decimal fraction of reflection of the dyed fabric; K, absorption coefficient; S, scattering coefficient; N, Nanoparticles form of the compound.

Table 2 In vitro antimicrobial activity of the newly synthesized compounds against bacterial and fungi species

Compd. number	Mean diameter of inhibition zone (mm)				
	Bacterial species				Fungal strain
	Gram-positive bacterial strain		Gram-negative bacterial strain		
	Bacillus subtilis (ATCC 6633)	*Staphylococcus aureus* (ATCC 29,213)	*Escherichia coli* (ATCC 25,922)	*Pseudomonas aeruginosa* (ATCC 27,853)	*Aspergillus niger* (RCMB 002568)
2a	9±0.19	0.00	0.00	0.00	0.00
2b	15±0.48	12±0.19	0.00	12±0.20	0.00
2bN	24±0.62	19±0.24	15±0.65	22±0.64	13±0.22
2c	12±0.34	10±0.48	14±0.20	13±0.33	0.00
2cN	18±0.14	15±0.96	20±0.64	19±0.27	14±0.20
2d	0.00	0.00	0.00	14±0.72	0.00
2e	13±0.63	0.00	0.00	0.00	0.00
2f	16±0.20	10±0.96	0.00	0.00	0.00
2fN	22±0.47	23±0.62	21±0.34	25±0.28	19±0.32
2g	14±0.27	15±0.34	0.00	10±0.48	0.00
2gN	21±0.23	24±0.33	13±0.54	18±0.34	16±0.18
2h	16±0.33	11±0.27	12±0.72	10±0.63	15±0.27
2hN	22±0.23	17±0.15	19±0.44	16±0.39	20±0.18
2i	11±0.20	13±0.48	16±0.27	17±0.34	0.00
2j	10±0.96	0.00	0.00	0.00	0.00
5a	0.00	0.00	0.00	0.00	0.00
5b	9±0.34	0.00	12±0.96	0.00	0.00
Tetracycline (standard)	25±0.46	25±0.34	23±0.72	20±0.63	-
Amphotericin B (standard)	-	-	-	-	22±0.34

Notes: Solvent used: DMSO solution. Data are expressed as mean ± SEM of three independent experiments performed in duplicates. -, Indicates not tested.

methane (2.24 g, 0.01 mol) in sodium acetate solution (0.50 g) was added. A mixture of any of the later arylhydrazono (0.01 mol) in sodium ethoxide solution (0.68 g, 0.01 mol) and cyanoacetamide (0.84 g, 0.01 mol) was added. The mixture was refluxed for 3 hrs and then allowed to cool. Acidified solution with cold dilute

Table 3 The minimal inhibitory concentrations (MIC) of the synthesized compounds against pathogenic bacteria and fungi

Compd. number	The minimum inhibitory concentration (MIC) (μg/mL)				
	Bacterial species				Fungal strain
	Gram-positive bacterial strain		Gram-negative bacterial strain		
	Bacillus subtilis (ATCC 6633)	*Staphylococcus aureus* (ATCC 29,213)	*Escherichia coli* (ATCC 25,922)	*Pseudomonas aeruginosa* (ATCC 27,853)	*Aspergillus niger (RCMB 002568)*
2b	7.81	125.00	0.00	15.62	0.00
2bN	5.02	62.50	31.25	7.81	166.6
2c	125.00	250.00	31.25	62.50	0.00
2cN	62.50	142.85	27.77	31.15	142.85
2fN	166.6	15.62	1.95	0.97	7.81
2g	31.25	15.62	0.00	125.00	0.00
2gN	7.81	3.90	15.62	62.50	83.33
2h	3.90	62.50	15.62	31.25	125.00
2hN	3.90	31.25	7.81	15.62	18.51
2i	250.00	31.25	3.90	1.95	0.00
Tetracycline (standard)	31.30	62.50	15.60	62.50	-
Amphotericin B (standard)	-	-	-	-	62.50

Notes: (-) indicates not tested. Tetracycline and Amphotericin B were used as standards against the tested bacteria and fungi, respectively.

hydrochloric acid was added then the final solid product was collected by filtration and crystallized from ethanol.

5-((4-Cholrophenyl)diazenyl)-4-methyl-2-oxo-6-phenyl-1,2-dihydropyridine-3-carbonitrile (2a)

Orange crystals; yield: 90% (3.14 g), mp: 238–240°C; IR (KBr, ν cm^{-1}): 3465, 3147 (NH), 3059 (CH-aromatic), 2982, 2927 (CH_3), 2207 (CN), 1630 (C=O), 1554, 1443 (C=C). ^{1}H-NMR (DMSO-d_6) δ: 2.62 (s, 3H, CH_3), 7.19–7.47 (m, 9H, C_6H_4, C_6H_5), 8.60 (s, 1H, NH). ^{13}C-NMR (DMSO-d_6) δ: 21.1, 98.3, 119.9, 123.0, 127.2, 127.8, 127.8, 128.1, 128.1, 129.4, 129.4, 130.7, 130.7, 132.0, 132.9, 141.4, 146.0, 165.2, 170.5. MS (EI): *m/z* (%) 349 $[M]^+$ (3.94), 57 (100.00). *Anal*. Calcd. for $C_{19}H_{13}N_4OCl$ (348.79): C, 65.43; H, 3.76; N, 16.06. Found: C, 65.01; H, 4.16; N, 16.40.

5-((4-Bromophenyl)diazenyl)-4-methyl-2-oxo-6-phenyl-1,2-dihydropyridine-3-carbonitrile (2b)[49]

4-Methyl-5-((4-nitrophenyl)diazenyl)-2-oxo-6-phenyl-1,2-dihydropyridine-3-carbonitrile (2c)

Dark red crystals; yield: 94% (3.22 g); mp: 254–256°C; IR (KBr, ν cm^{-1}): 3473 (OH, NH), 3044 (CH-aromatic), 2925 (CH_3), 2270 (CN), 1620 (C=O), 1588, 1459 (C=C), 1563 (N=N). ^{1}H-NMR (DMSO-d_6) δ: 2.70 (s, 3H, CH_3), 7.26–7.51 (m, 9H, C_6H_4, C_6H_5), 8.23 (s, 1H, NH). ^{13}C-NMR (DMSO-d_6) δ: 21.7, 98.2, 117.0, 120.0, 122.2, 122.2, 125.3, 125.3, 126.0, 127.3, 127.3, 130.8, 130.8, 134.5, 134.9, 146.2, 155.0, 162.0, 170.2. MS (EI): *m/z* (%) 359 $[M]^+$ (1.00), 323 (100.00). *Anal*. Calcd. for $C_{19}H_{13}N_5O_3$ (359.34): C, 63.51; H, 3.65; N, 19.49. Found: C, 63.21; H, 3.35; N, 19.19.

5-((2,4-Dichlorophenyl)diazenyl)-4-methyl-2-oxo-6-phenyl-1,2-dihydropyridine-3-carbonitrile (2d)

Dark brown crystals; yield: 92% (3.53 g); mp: 190–192°C; IR (KBr, ν cm^{-1}): 3457, 3195 (OH, NH), 3078 (CH-aromatic), 2927 (CH_3), 2211 (CN), 1647 (C=O), 1558, 1441 (C=C), 1508 (N=N). ^{1}H-NMR (DMSO-d_6) δ: 2.68 (s, 3H, CH_3), 6.62–7.64 (m, 8H, C_6H_3, C_6H_5), 7.70 (s, 1H, NH). ^{13}C-NMR (DMSO-d_6) δ: 22.0, 100.0, 118.1, 127.2, 127.8, 127.8, 128.3, 129.6, 129.6, 129.9, 130.8, 132.4, 132.6, 132.8, 133.4, 133.4, 148.7, 149.0, 170.0. MS (EI): *m/z* (%) 383 $[M]^+$ (10.34), 360 (100.00). *Anal*. Calcd. for $C_{19}H_{12}N_4OCl_2$ (383.23): C, 59.55; H, 3.16; N, 14.62. Found: C, 59.22; H, 3.13; N, 14.33.

5-((2,4-Dimethoxyphenyl)diazenyl)-4-methyl-2-oxo-6-phenyl-1,2-dihydropyridine-3-carbonitrile (2e)[49]

5-((4-Chlorophenyl)diazenyl)-2-oxo-4,6-diphenyl-1,2-dihydropyridine-3-carbonitrile (2f)

Orange crystals; yield: 93% (3.82 g); mp: 273–275°C; IR

(KBr, ν cm^{-1}): 3450 (OH, NH), 3030 (CH-aromatic), 2226 (CN), 1650 (C=O), 1568, 1442 (C=C), 1536 (N=N). ^{1}H-NMR (DMSO-d_6) δ: 6.94–7.57 (m, 14H, C_6H_4, $2C_6H_5$), 7.99 (s, 1H, NH), 13.37 (s, 1H, OH enol form). ^{13}C-NMR (DMSO-d_6) δ: 99.1, 115.5, 115.7, 123.5, 125.1, 128.3, 128.3, 128.6, 128.6, 128.7, 128.7, 129.0, 129.0, 129.9, 129.9, 130.9, 130.9, 132.1, 134.1, 134.2, 134.7, 150.4, 160.1, 170.2. MS (EI): *m/z* (%) 413 $[M+2]^+$ (3.46), 412 $[M+1]^+$ (19.29), 411 $[M]^+$ (41.72), 410 $[M-1]^+$ (47.61), 409 $[M-2]^+$ (100.00). *Anal*. Calcd. for $C_{24}H_{15}N_4OCl$ (410.86): C, 70.16; H, 3.68; N, 13.64. Found: C, 69.80; H, 3.83; N, 13.86.

5-((4-Bromophenyl)diazenyl)-2-oxo-4,6-diphenyl-1,2-dihydropyridine-3-carbonitrile (2g)

Golden brown crystals; yield: 88% (4.01 g); mp: 286–288°C; IR (KBr, ν cm^{-1}): 3434 (OH, NH), 3029 (CH-aromatic), 2225 (CN), 1649 (C=O), 1568, 1463 (C=C), 1533 (N=N). ^{1}H-NMR (DMSO-d_6) δ: 6.86–7.57 (m, 14H, C_6H_4, $2C_6H_5$), 7.59 (s, 1H, NH), 13.31 (s, 1H, OH enol form). ^{13}C-NMR (DMSO-d_6) δ: 98.1, 115.7, 115.8, 123.8, 125.0, 127.6, 128.3, 128.3, 128.6, 128.6, 129.0, 129.0, 129.3, 129.3, 131.0, 131.0, 132.8, 132.8, 133.0, 134.5, 135.8, 150.7, 160.0, 171.1. *Anal*. Calcd. for $C_{24}H_{15}N_4OBr$ (455.31): C, 63.31; H, 3.32; N, 12.31. Found: C, 63.01; H, 3.39; N, 12.62.

5-((4-Nitrophenyl)diazenyl)-2-oxo-4,6-diphenyl-1,2-dihydropyridine-3-carbonitrile (2h)

Golden brown crystals; yield: 95% (4.00 g); mp: 296–298°C; IR (KBr, ν cm^{-1}): 3435, 3237 (OH, NH), 3033 (CH-aromatic), 2226 (CN), 1651 (C=O), 1603, 1464 (C=C), 1524 (N=N). ^{1}H-NMR (DMSO-d_6) δ: 7.08–7.59 (m, 14H, C_6H_4, $2C_6H_5$), 8.22 (s, 1H, NH)0,13.50 (s, 1H, OH enol form). ^{13}C-NMR (DMSO-d_6) δ: 99.1, 115.1, 115.5, 122.7, 122.7, 125.5, 125.5, 127.8, 127.9, 128.3, 128.3, 128.4, 128.4, 128.7, 128.7, 129.1, 129.1, 131.1, 134.3, 134.5, 148.5, 154.9, 160.1, 169.2. MS (EI): *m/z* (%) 420 $[M-1]^+$ (9.89), 421 $[M]^+$ (10.27), 409 (100.00). *Anal*. Calcd. for $C_{24}H_{15}N_5O_3$ (421.41): C, 68.40; H, 3.59; N, 16.62. Found: C, 68.60; H, 3.99; N, 16.99.

5-((2,4-Dichlorophenyl)diazenyl)-2-oxo-4,6-diphenyl-1,2-dihydropyridine-3-carbonitrile (2i)

Golden brown crystals; yield: 89% (3.96 g); mp: 267–269°C; IR (KBr, ν cm^{-1}): 3439 (OH, NH), 3031 (CH-aromatic), 2224 (CN), 1652 (C=O), 1569, 1459 (C=C), 1532 (N=N). ^{1}H-NMR (DMSO-d_6) δ: 7.35–8.02 (m, 13H, C_6H_3, $2C_6H_5$), 8.19 (s, 1H, NH). ^{13}C-NMR (DMSO-d_6) δ: 96.1, 115.7, 118.2, 123.8, 126.1, 127.1, 128.3, 128.3, 128.5, 128.5, 128.8, 128.8, 129.1, 129.1, 130.1, 131.0, 132.8, 134.1, 135.2, 135.7, 135.7, 136.6, 160.3, 169.1. MS (EI): *m/z* (%) 443 $[M-2]^+$ (100.00), 444 $[M-1]^+$ (57.54), 445 $[M]^+$ (73.23), 446 $[M+1]^+$ (39.05), 447 $[M+2]^+$ (18.68), *Anal*. Calcd. for $C_{24}H_{14}N_4OCl_2$ (445.30): C, 64.73; H, 3.17; N, 12.58. Found: C, 64.50; H, 3.35; N, 12.89.

5-((2,4-Dimethoxyphenyl)diazenyl)-2-oxo-4,6-diphenyl-1,2-dihydropyridine-3-carbonitrile (2j)

Light golden brown crystals; yield: 90% (3.93 g); mp: 274–276°C; IR (KBr, ν cm^{-1}): 3300 (OH, NH), 3026 (CH-aromatic), 2926, 2852 (CH_3), 2225 (CN), 1650 (C=O), 1570, 1460 (C=C), 1535 (N=N). ^{1}H-NMR (DMSO-d_6) δ: 3.50 (2s, 6H, $2CH_3$), 6.86–7.58 (m, 13H, C_6H_3, $2C_6H_5$), 7.62 (s, 1H, NH), 13.36 (s, 1H, OH enol form). ^{13}C-NMR (DMSO-d_6) δ: 55.1, 55.1, 91.5, 98.3, 98.5, 106.5, 115.7, 118.2, 123.8, 126.2, 128.3, 128.3, 128.6, 128.6, 128.8, 128.8, 130.5, 130.5, 130.9, 132.9, 134.1, 134.8, 159.2, 160.0, 161.5, 169.4. MS (EI): *m/z* (%) 344 (100.00), 434 $[M-2]^+$ (0.79), 437 $[M+1]^+$ (1.82), 438 $[M+2]^+$ (2.12). *Anal*. Calcd. for $C_{26}H_{20}N_4O_3$ (436.46): C, 71.55; H, 4.62; N, 12.84. Found: C, 71.20; H, 4.36; N, 13.10.

5-((1,5-Dimethyl-3-oxo-2-phenyl-2,3-dihydro-1*H*-pyrazol-4-yl)diazenyl)-4-methyl-2-oxo-6-phenyl-1,2-dihydropyridine-3-carbonitrile (5a)

Dark red crystals; yield: 84% (3.57 g); mp: 253–255°C; IR (KBr, ν cm^{-1}): 3436 (OH, NH), 3055 (CH-aromatic), 2921, 2855 (CH_3), 2200 (CN), 1659, 1639 (2C=O), 1591, 1450 (C=C), 1526 (N=N). ^{1}H-NMR (DMSO-d_6) δ: 2.51, 3.08, 3.35 (3s, 9H, $3CH_3$), 7.35–7.88 (m, 10H, $2C_6H_5$), 7.71 (s, 1H, NH). ^{13}C-NMR (DMSO-d_6) δ: 10.5, 13.1, 36.3, 99.1, 101.1, 115.5, 117.1, 123.3, 125.0, 125.0, 125.6, 126.8, 127.2, 172.2, 128.3, 128.3, 129.5, 129.5, 134.8, 135.3, 159.5, 160.5, 160.6, 169.5. *Anal*. Calcd. for $C_{24}H_{20}N_6O_2$ (424.45): C, 67.91; H, 4.75; N, 19.80. Found: C, 68.20; H, 4.60; N, 19.99.

5-((1,5-Dimethyl-3-oxo-2-phenyl-2,3-dihydro-1*H*-pyrazol-4-yl)diazenyl)-2-oxo-4,6-diphenyl-1,2-dihydropyridine-3-carbonitrile (5b)

Dark orange crystals; yield: 93% (4.52 g); mp: 245–247°C; IR (KBr, ν cm^{-1}): 3433 (OH, NH), 3059 (CH-aromatic), 2925, 2855 (CH_3), 2200 (CN), 1660, 1641 (2C=O), 1587, 1410 (C=C). ^{1}H-NMR (DMSO-d_6) δ: 1.79, 2.97 (2s, 6H, $2CH_3$), 7.30–7.56 (m, 15H, $3C_6H_5$),

7.58 (s, 1H, NH). MS (EI): *m/z* (%) 415 (100.00), 487 $[M+1]^+$ (1.20). *Anal*. Calcd. for $C_{29}H_{22}N_6O_2$ (486.52): C, 71.95; H, 4.56; N, 17.27. Found: C, 71.60; H, 4.63; N, 16.98.

SeNPs

In Erlenmeyer flask, 5 mL from each organic compound number **2b, 2c, 2f, 2g**, and **2h**, mixed with 5 mL from 1 mM Selenious acid and kept at room temperature for 24 hrs under stirring condition. The absorption spectrum of the sample was recorded on JASCO V-560 UV-visible spectrometer operating at a resolution of 1 nm with a slight modification of this method according to the reported method.[50] The aqueous Se^{2+} ions (1 mM) were reduced to SeNPs when added to organic compound number **2b, 2c, 2f, 2g**, and **2h**. This is indicated by the color change into reddish and the control showed no color change.

Methods for characterization of SeNPs

SeNPs were characterized by UV-Visible spectrophotometry and DLS, TEM analysis, and XRD.

UV-Vis

UV-Visible Spectra of SeNPs were recorded as a function of wavelength from 200 to 900 nm at a resolution of 1 nm.

DLS

Average particle size and size distribution were determined and before measurements, the samples were diluted 10 times with de-ionized water. 250 µL of suspension was transferred to a disposable low volume cuvette. After equilibration to a temperature 25°C for 2 mins, five measurements were performed using 12 runs of 10 s each.

TEM

The size and morphology of the synthesized nanoparticles were recorded by using TEM. TEM studies were prepared by drop coating SeNPs onto carbon-coated TEM grids. The Film on the TEM grids was allowed to dry, the extra solution was removed using a blotting paper.

XRD

For XRD analysis, the adjusted sample was centrifuged, and the precipitate was dried under vacuum and taken for XRD analysis. XRD patterns were obtained with the XRD-6000 series, including stress analysis, residual austenite quantitation, crystallite size/lattice strain, crystallinity calculation, material analysis via overlaid XRD pattern Shimadzu apparatus using nickel-filter and Cu-Ka target, SSI, Kyoto, Japan. The average crystalline size of the NPs can also be determined using Debye–Scherrer equation: $\mathbf{D=k\lambda/\beta\ Cos\ \theta}$. Where **D** is the average crystalline size (nm), **k** is the Scherrer constant with the value from 0.9 to 1λ is the X-ray wavelength, β is the full width of half maximum and θ is the Bragg diffraction angle (degrees).

Spectral characterization, color assessment, and dyeing properties

Dyeing procedure

The dyeing process was performed by using a solution containing 5% dye (based on the weight of sample), ammonium persulphate at 120°C for 45 mins and 2 g/L dispersing agent. The solution of the dye was adjusted at Ph=4.5–5 by using acetic acid. In the end of dyeing time, a solution containing 5 g/L detergent was used to wash the fabric sample for several times. Finally, the fabric sample was rinsed with water and dried at ambient conditions. The color of the dyes on nylon 66 fibers is indicated[51] (Table 1).

Color strength

At λ_{max}=400 nm, the color strength of the dyed samples was measured and expressed as (K/S) (Table 1).

Fastness properties

According to the standard method,[52] the color fastness to washing, rubbing (dry and wet crocking), and perspiration was determined (Table 1).

Colorfastness to washing testing

The colorfastness to washing test was occurred in accordance with test method (ISO 105-C01- 1989). Evaluation of the wash fastness was determined by using the Gray-scale for color change (Table 1).

Colorfastness to rubbing testing

This test is evaluated the degree of the color, which may be transferred from the colored fabric surface to another surface, by rubbing. Color fastness to rubbing test involving dry crocking test and wet crocking test which occurred by test method (ISO 105-X12/2001).

Colorfastness to perspiration testing

In this test, two artificial perspiration solutions were prepared (acidic solution and alkaline solution). The color fastness to perspiration test was occurred in accordance with test method (ISO 105–E 0 4-1994 –

cor1/2002). The effect on the color was expressed and defined by reference to Gray-scale for color change.

Colorfastness to light testing

The light fastness test was occurred in accordance with test method AATCC Test Method 16 by using artificial light source, namely Xenon Arc lamp exposure as it is representative of natural daylight for 40 hrs. The effect on the color of the test samples was expressed by using color change Gray-scale 1–5.

Test microorganisms

The test microorganisms were used in the present study, Gram-positive, (*Bacillus subtilis* ATCC 6633, *Staphylococcus aureus* ATCC 29213). Gram-negative (*Pseudomonas aeruginosa* ATCC 27853, *Escherichia coli* ATCC 25922). Also, *Aspergillus niger* (RCMB 002568) were used to define the antifungal activity of the synthesized compounds.

Antimicrobial activity

The antimicrobial potential of newly synthesized compounds was investigated toward the test microorganisms and expressed as the diameter of the inhibition zones (as shown in Table 2), according to the agar plate diffusion method.[53] Briefly, 100 µL of the test bacteria/fungi was grown in 10 mL of fresh media until they reached a count of approximately 10^8 cells/mL for bacteria or 10^5 cells/mL for fungi. One mL of each sample (at 0.5 mg/mL) was added to each well (10 mm diameter holes cut in the agar gel). The plates were incubated for 24 hrs at 37°C (for bacteria and yeast) and for 72 hrs at 27°C (for filamentous fungi), after incubation, the microorganism's growth was observed. Tetracycline was used as standard antibacterial drugs while amphotericin B was used as standard antifungal drug. The resulting inhibition zone diameters were measured in millimeters and used as criterion for the antimicrobial activity. Solvent controls (DMSO) were included in every experiment as negative controls. DMSO was used for dissolving the tested compounds and showed no inhibition zones, confirming that it has no influence on growth of the tested microorganisms.

MIC of the active compounds

The MIC of the most potent synthesized compounds were determined (as shown in Table 3), by the conventional paper disk diffusion method,[54] by applying paper disk (266812 W. Germany 12.7 mm in diameters). Bacteria were grown on nutrient agar medium, while fungi and yeast were grown on Sabouraud agar medium. The purified synthesized compounds were dissolved in water and loaded on paper disks with different concentrations as the following (250, 125, 62.50, 31.25, 15.62, 7.81, 3.90, 1.95, 0.98, 0.49, 0.24, and 0.12 µg/mL). Drying disks were loaded on the surface of agar plates inoculated with test organism. Growth inhibition was examined after 24 hrs. from incubation at 37°C for bacteria and after 72 hrs. incubation at 27°C for fungi and yeast. Each test was repeated three times. MIC was expressed as the lowest concentration inhibiting test organism's growth.

Statistical analysis

The results were analyzed by using the software version 6.0 (Minitab 11.USA) and analysis of Variance (ANOVA analysis).

Results and discussion

Chemistry

In the current study, we are demonstrating the synthesis of novel polyfunctionalized heterocyclic compounds containing pyridinone moiety in the form of azo disperses dyes derivatives. The reaction of diazotized aniline derivatives or diazotized amino antipyrene with benzoyl acetone or dibenzoyl methane in sodium ethoxide afforded aryl hdrazo derivatives **1a–j** and **4a–b,** respectively. The latter in the same reaction mixture reacted with cyanoacetamide in sodium ethoxide by losing two molecules of water then follow 1,5-proton shift gave the dihydropyridine-3-carbonitrile derivatives **2a–j** (Figure 1) and **5a–b** (Figure 2), respectively. The structure of compound **2a** was confirmed on the basis of analytical and spectral data. Thus, the ^{1}H-NMR spectrum showed the presence of singlet at δ 2.62 ppm for the presence of CH_3 moiety, multiplets at δ 7.19–7.47 ppm for two phenyl groups, and singlet at δ 8.60 ppm for the NH group. Moreover, the mass spectrum revealed m/z at 349 for molecular ion peak. Also, the structure of compound **2f** was confirmed through ^{1}H-NMR spectrum which showed multiplets at δ 6.94–7.57 ppm for the two phenyl moieties, singlet at δ 7.99 ppm for NH group and 13.37 ppm for the OH moiety. The mass spectrum showed m/z at 411 $[M]^+$. The presence of the OH group in infrared at ν=3450 cm^{-1}, cyano group at ν=2226 cm^{-1} and C=O

at v=1650 cm^{-1} confirmed the presence of tautomeric keto-Enol form structures. Some of the newly synthesized compounds were appeared in the enol form beside the keto form such as **2f, 2g, 2h, 2j**. The ^{1}H-NMR spectra of the previous compounds indicate the presence of the OH groups at δ=13.37 ppm for compound **2f**, 13.31 ppm for **2g**, 13.50 ppm for **2h** and 13.36 ppm for **2j**. Also, the IR spectra of the enol form for the previous compounds showed the presence of the OH group in the range v=3300–3450 cm^{-1}. On the other hand, all the prepared compounds tested for the synthesis of SeNPs only five compounds **2b, 2c, 2f, 2g**, and **2h** gave positive result which indicated by the color change into reddish and the control showed no color change. Only the five compounds **2b, 2c, 2f, 2g,** and **2h** with its (SeNps) were tested to determine their characterizations after dyeing process. The characterizations of the dyed fabrics were evaluated by the measurement of color strength (expressed as K/S) and the measurement of fastness properties by determining the wash, rub, perspiration, and light fastness. Also, SeNPs were characterized by UV-Visible spectrophotometry, DLS, X-RD, and TEM analysis. Moreover, the antimicrobial activity for all the synthesized compounds besides the five (SeNPs) compounds were evaluated and indicate that compounds **2b, 2bN, 2c, 2cN, 2f, 2fN, 2g, 2gN, 2h, 2hN, 2i**, and **5b** were the most active compounds toward the two bacterial species. Also, all the (SeNPs) synthesized compounds and compound **2h** revealed higher antifungal activity toward the fungal strain. Also, the MIC test was performed on the most active compound. By comparing the reactivity of the (SeNPs) synthesized compounds and the other prepared azo disperse dyes compounds, we deduced that all the (SeNPs) synthesized compounds revealed higher antimicrobial activity toward bacterial and fungal species than the other synthesized compounds. From the other side, the fastness properties for the (SeNPs) synthesized products almost equal with that for the other prepared pyridine azo dye compounds except fastness for rubbing which indicate higher fastness in case of (SeNPs) synthesized compounds.

Characterization of SeNPs

UV-Vis

The dispersion of SeNPs displays intense colors due to the Plasmon resonance absorption. The surface of a metal is like plasma, having free electrons in the conduction band and positively charged nuclei. Therefore, metallic nanoparticles have characteristic of optical absorption spectrum in the UV-Visible region. UV-Visible spectrum of SeNPs synthesized by organic compounds number **2b, 2c, 2f, 2g,** and **2h** at room temperature have spectrum at λ_{max} at 430, 440, 435, 445, and 455 nm, respectively, as shown in Figures S1–S5 which exhibits the maximum absorption of prepared silver nanoparticles at 0.793, 0.719, 2.597, 0.850, and 2.262, respectively.

DLS

The average particle size was determined by DLS method and was found to be 29.8, 31.5, 23.1, 36.3, and 45.3 nm, respectively, as shown in Figures S6–S10 for SeNPs of organic compounds number **2b, 2c, 2f, 2g**, and **2h,** respectively at room temperature.

TEM

TEM examination of the solution containing SeNPs which synthesized by organic compounds number **2b, 2c, 2f, 2g**, and **2h,** respectively at room temperature, demonstrated spherical particles within nano ranged from 31.5 to 51.22 nm as shown in Figures 3–7.

XRD

XRD pattern for the SeNPs was presented in Figure 8. Several peaks are observing, these being at selenium nanocomposite show the diffraction features appearing at nine theta (degree) as 23.2°, 30.5°, 41.7°, 44.3°, 46.4°, 52.3°, 56.7°, 62.5°, and 72.6°. These correspond to the (100), (101), (110), (102), (111), (201), (113), (202), and (210) planes of the standard cubic phase of Se, respectively. The XRD pattern indicated that SeNPs were in the face-centered cubic) structure and crystal in nature. The observation of diffraction peaks for the SeNPs indicates that these are crystalline in this size range while its refining is related to the particles in the nanometer size regime.

Color assessment and dyeing properties

The newly synthesized dyes were applied to nylon 66 fabrics at 5% dye (based on the weight of sample) by the standard method and gave generally different colors on the dyed fabrics. The estimation fastness shades of the dyed fabrics were analyzed and tests by Gray-scale for color change, the results were expressed in terms of color ratings 1–5 (Table 1). By comparing the results which showed for azo dyes and its SeNPs, in general, the data revealed that rubbing fastness of the

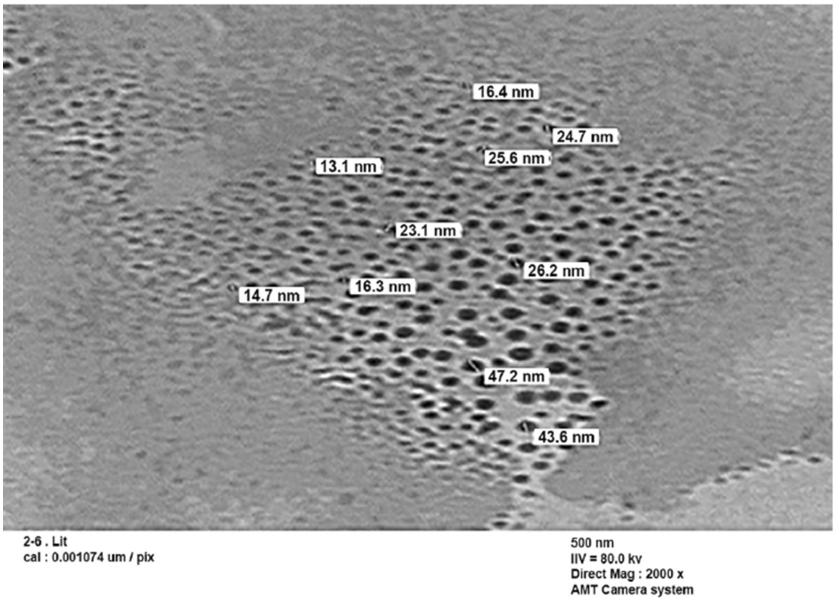

Figure 3 TEM image for selenium nanoparticles synthesized by using compound **2b** at room temperature.
Abbreviation: TEM, transmission electronmicroscope.

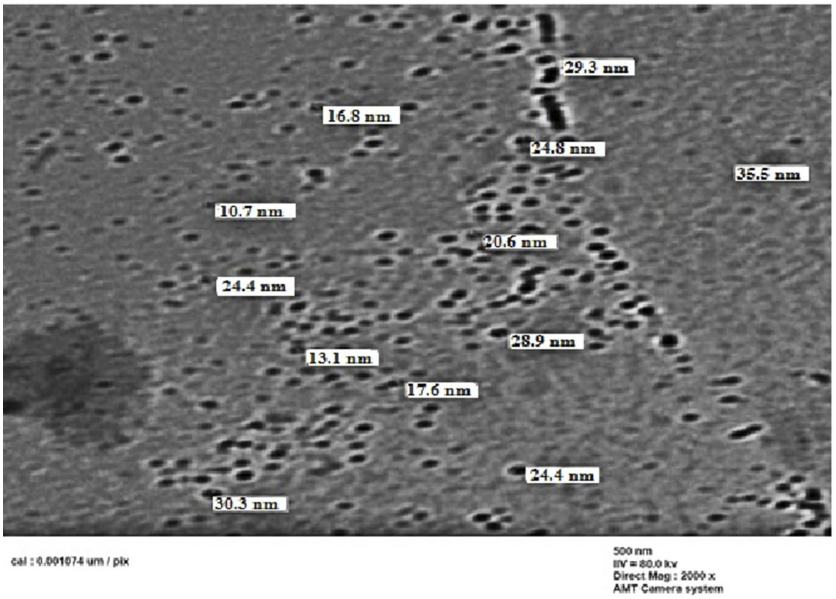

Figure 4 TEM image for selenium nanoparticles synthesized by using compound **2c** at room temperature.
Abbreviation: TEM, transmission electron microscope.

compounds, assessed in terms of dry and wet, indicated good fastness to rubbing for both dry and wet for SeNPs dyes number **2bN, 2fN, 2gN**, and **2hN**. Wash fastness ratings for change in color are good for dyes number **2f, 2fN, 2g, 2gN**, and **2h**. Perspiration fastness properties (acidic and alkaline) of the dyed samples in terms of ratings for staining of adjacent fabrics and change are good for dyes number **2b, 2bN, 2c, 2g**, and **2gN** which indicated the stability of the dyes toward degradation under either acidic or basic conditions. Also, light fastness for most of the synthesized dyes was of a generally of good order.

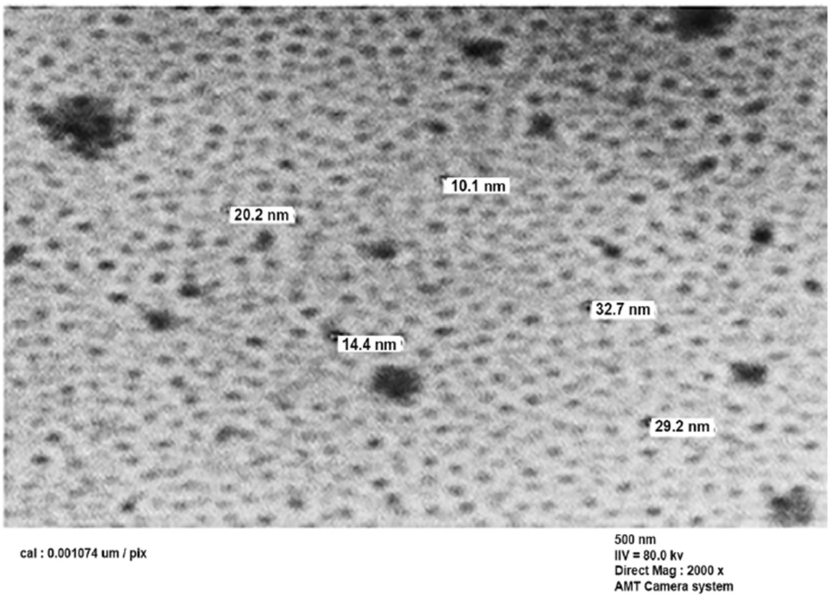

Figure 5 TEM image for selenium nanoparticles synthesized by using compound **2f** at room temperature.
Abbreviation: TEM, transmission electron microscope.

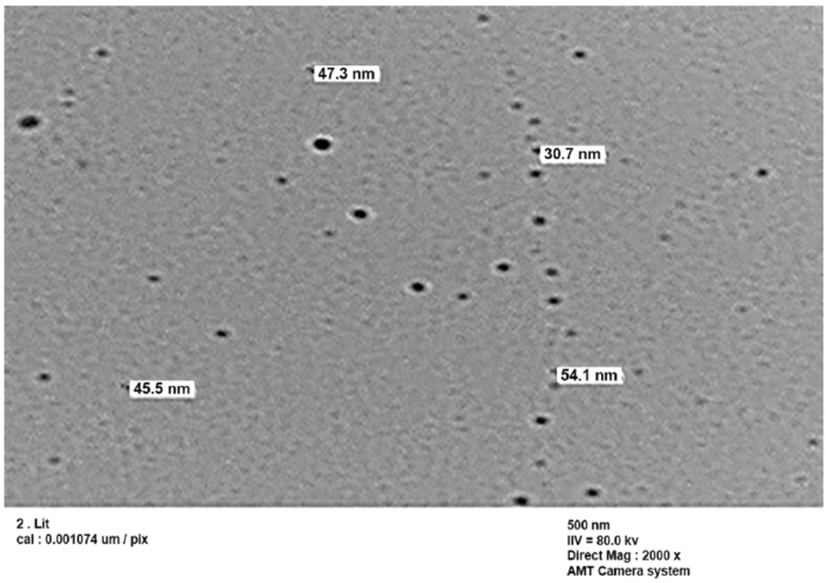

Figure 6 TEM image for selenium nanoparticles synthesized by using compound **2g** at room temperature.
Abbreviation: TEM, transmission electron microscope.

Antimicrobial activity

All the synthesized dyes are tested against bacterial and fungal species which indicate that compounds **2b, 2bN, 2c, 2cN, 2f, 2fN, 2g, 2gN, 2h, 2hN, 2i**, and **5b** were the most active compounds toward G+ and G− bacterial species, while compounds **2bN, 2cN, 2fN, 2gN, 2h,** and **2hN** were the most active against fungal strain. The MIC of the most active compounds (**2b, 2bN, 2c, 2cN, 2fN, 2g, 2gN,**

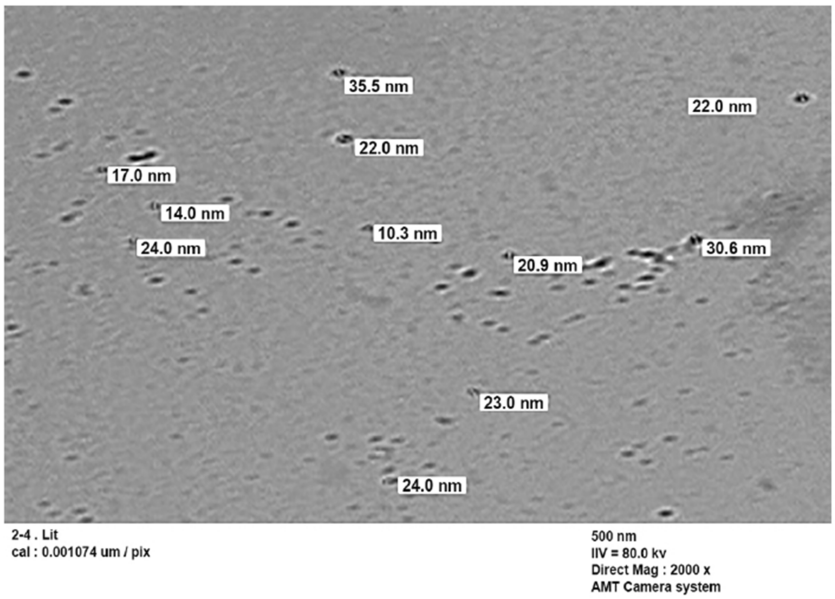

Figure 7 TEM image for selenium nanoparticles synthesized by using compound **2h** at room temperature.
Abbreviation: TEM, transmission electron microscope.

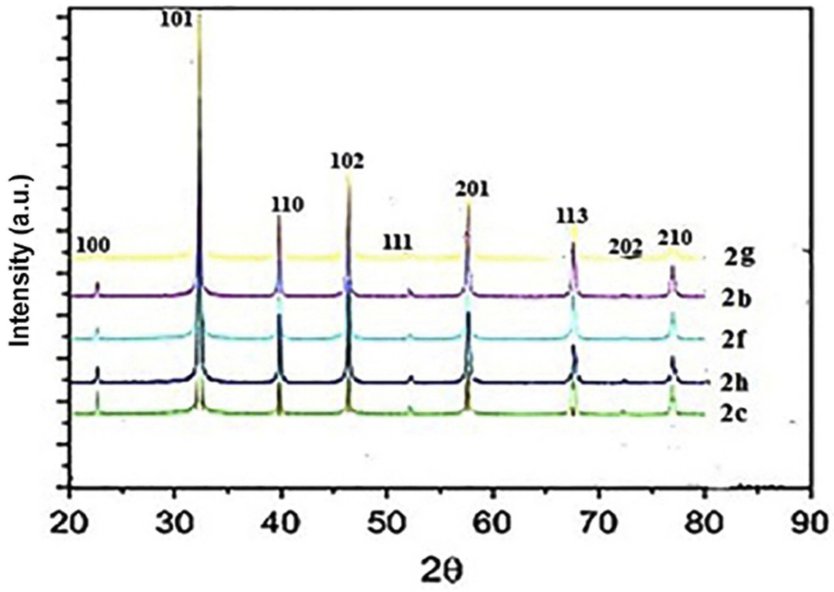

Figure 8 XRD pattern for the selenium nanoparticles synthesized by using compound (**2b, 2c, 2f, 2g**, and **2h**) at room temperature.
Abbreviation: XRD, X-Ray diffraction.

2h, 2hN, and **2i**) against Gram-positive, Gram-negative bacterial species and fungal strain was evaluated. We conclude from this study that all the SeNPs synthesized compounds revealed higher antimicrobial activity than the other prepared compounds.

Conclusion

The objective of the present work was to prepare a variety and novel of pyridine azo disperse dye derivatives with antibacterial activity and their SeNPs with good fastness properties. The reaction of diazotized aniline derivatives or

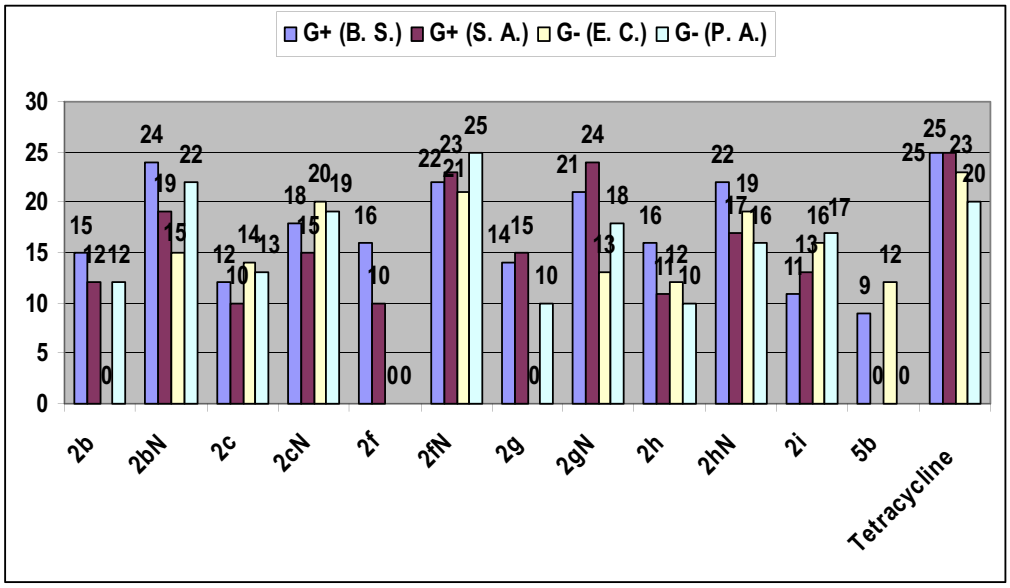

Figure 9 The most active synthesized compounds against Gram-positive and Gram-negative bacterial species.

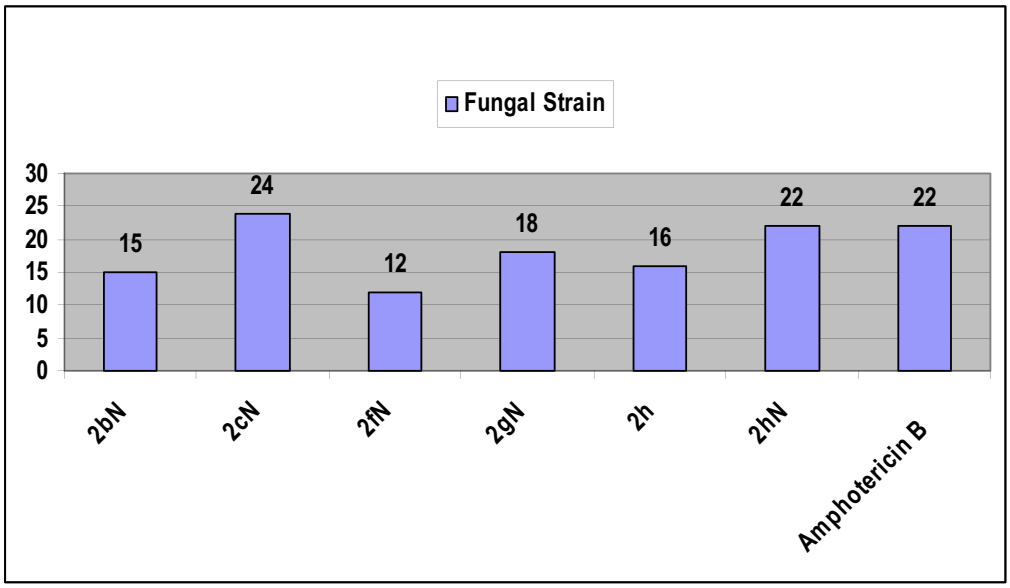

Figure 10 The activity of the synthesized compounds against fungal strain.

diazotized amino antipyrene and cyanoacetamide with any of dibenzoyl methane or benzoyl acetone in strong basic medium sodium ethoxide afforded the pyridine azo dye derivatives. The study of the dyeing characteristics of the newly synthesized compounds and its (SeNPs), on nylon 66 fabrics, revealed high color strength, good wash fastness, good rub fastness, good perspiration as well as good light fastness. The prepared (SeNPs) compounds were characterized by UV spectrophotometry (DLS), (XRD), and (TEM) analysis. The antibacterial activity of the new novel products revealed that compounds **2b, 2bN, 2c, 2cN, 2f, 2fN, 2g, 2gN, 2h, 2hN, 2i**, and **5b** were the most active compounds toward all and some (at least two strains) of the Gram-positive and Gram-negative bacterial strains. Also, compounds **2bN, 2cN, 2fN, 2gN, 2h**, and **2hN** showed higher antifungal activity. Moreover, the MIC for the most active compounds was evaluated. As a result of the study, all the (SeNPs) synthesized compounds revealed

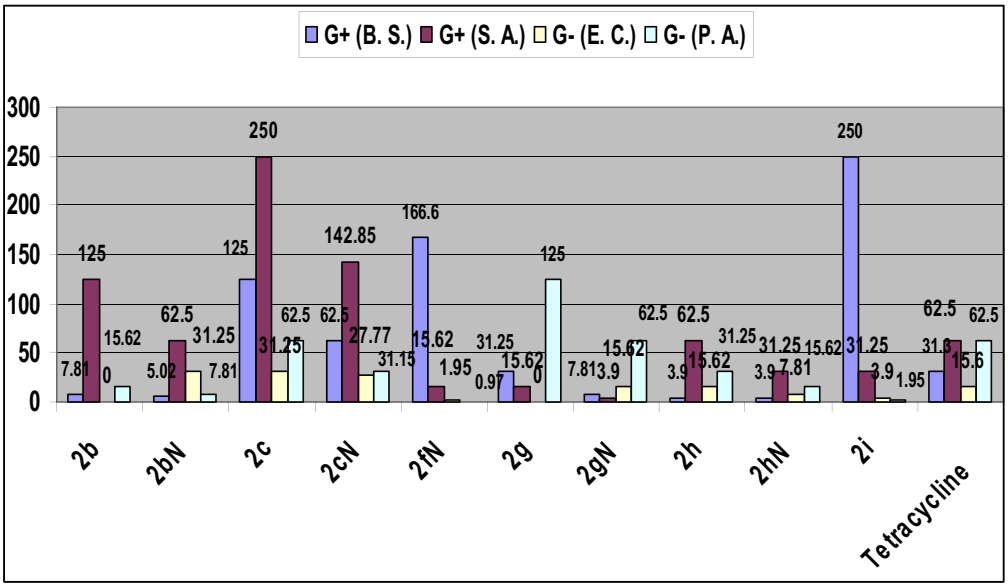

Figure 11 The Minimum Inhibitory Concentration (MIC) of the most active compounds against Gram-positive and Gram-negative bacterial species.

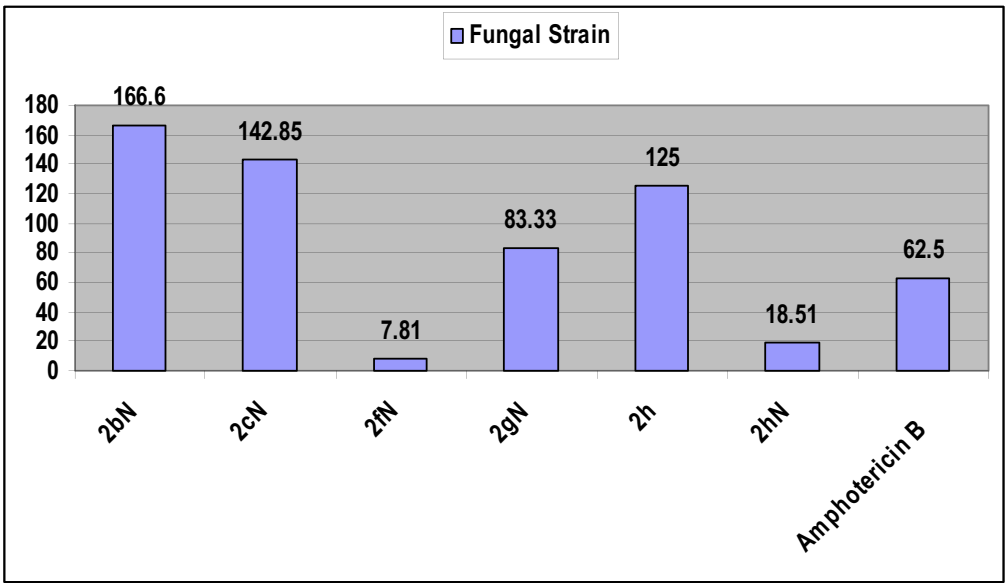

Figure 12 The Minimum Inhibitory Concentration (MIC) of the synthesized compounds against fungal strain.

enhancing in their antimicrobial activity than the other synthesized compounds.

Acknowledgment

Professor Maher H. E. Helal and Associate Prof. Amira E. M. Abdallah would like to express his deepest thanks to Faculty of Science Helwan University for the financial support through the research project.

Author contributions

All authors conceived, designed and performed the experiments, analyzed the data, contributed reagents/materials/analysis tools, wrote and approved the final manuscript and agree to be accountable for all aspects of the work.

Disclosure

The authors report no conflicts of interest in this work.

References

1. Fadda AA, El-Habbal MM. Ring opening and transamination of pyridinium salt. *Indian J Chem*. 1986;25B(1):194–200.
2. Fadda AA, Elagizy SA. Synthesis of azodisperse dyes with pyridine ring for dyeing polyester fibres: Part II. *Indian J Fibre Text*. 1989;14 (1):177–187.
3. Fadda AA, Hanna MA, Girges MM. New dyestuffs for polyester fibres-synthesis and comparative tinctorial behaviour of 3-alkyl-4-arylliydrazone-*n*]-picolinol-2-pyrazolin-5-ones and their isomeric pyrid-3-and 4-yl analogues. *J Chem Technol Biotechnol*. 1992;55 (1):9–16. doi:10.1002/jctb.280550103
4. Fadda AA, Ali MM, Fouda A. Synthesis of 3-aryl-5-[6-(α-picolyl) rhodanines and 3-aryl-5-(2-pyridylmethylene)rhodanine and their dyeing performance on acetate and/or other of fibres. *Indian J Fibre Text*. 1993;18(1):151–155.
5. Fadda AA, Ali MM, Etman HA, Fouda A. Synthesis of 3-aryl-5-[2′ (α-pyridophthaionyl)rhodanines and their dyeing performance on acetate and/or other fibres. *Indian J Fibre Text*. 1995a;20(2):108–111.
6. Bach V, Hansen G, Lamm G, Sens R. Acylphenyl)azo]pyridone disperse dyes and their use. *Eur Pat*. 1991;Appl:413229.
7. Sakoma KJ, Bello KA, Yakubu MK. Synthesis of some azo disperse dyes from 1-substituted 2-hydroxy-6-pyridone derivatives and their colour assessment on polyester fabric. *Open J Appl Sci*. 2012;2:54–59. doi:10.4236/ojapps.2012.21006
8. Chien CC, Wang IJ. Synthesis of some pyridone azo dyes from 1-substituted 2-hydroxy-6- pyridone derivatives and their colour assessment. *Dyes Pigments*. 1991;15(1):69–82. doi:10.1016/0143-7208(91)87008-B
9. Ertan N, Gurkan P. Synthesis and properties of some azo pyridone dyes and their Cu(II) complexes. *Dyes Pigments*. 1997;33:137–147. doi:10.1016/S0143-7208(96)00044-7
10. Ashkar SM, El-Apasery MA, Touma MM, Elnagdi MH. Synthesis of some novel biologically active disperse dyes derived from 4-methyl-2,6-dioxo-1-propyl-1,2,5,6-tetrahydropyridine-3-carbonitrile as coupling component and their colour assessment on polyester fabrics. *Molecules*. 2012;17:8822–8831. doi:10.3390/molecules17088822
11. El-Sayed HA, Moustafa AH, El-Torky AE, Abd El-Salam EA. A series of pyridines and pyridine based sulfa-drug as antimicrobial agents: design, synthesis and antimicrobial activity. *Russ J Gen Chem*. 2017;87(10):2401–2408. doi:10.1134/S107036321710022X
12. Bhardwaj V, Noolvi MN, Jalhan S, Patel HM. Synthesis, and antimicrobial evaluation of new pyridine imidazo [2,1*b*]-1,3,4-thiadiazole derivatives. *J Saudi Chem Soc*. 2016;20(Suppl1):S406–S410. doi:10.1016/j.jscs.2012.12.007
13. Elkanzi NAA, Bakr RB, Ghoneim AA. Design, synthesis, molecular modeling study, and antimicrobial activity of some novel pyrano[2,3-*b*]pyridine and Pyrrolo[2,3-*b*]pyrano[2.3-*d*]pyridine derivatives. *J Heterocyclic Chem*. 2018;56(2):406–416. doi:10.1002/jhet.3412
14. El-Sayed EH, Fadda AA. Synthesis and antimicrobial activity of some novel bis polyfunctional pyridine, pyran, and thiazole derivatives. *J Heterocyclic Chem*. 2018;55(10):2251–2260. doi:10.1002/jhet.3276
15. Dang T, Nizamov IS, Salikhov RZ, et al. Synthesis and characterization of pyridoxine, nicotine and nicotinamide salts of dithiophosphoric acids as antibacterial agents against resistant wound infection. *Bioorg Med Chem*. 2019;27(1):100–109. doi:10.1016/j.bmc.2018.11.017
16. Badr MH, Rostom SAF, Radwan MF. Novel polyfunctional pyridines as anticancer and antioxidant agents. synthesis, biological evaluation and *in Silico* ADME-T study. *Chem Pharm Bull*. 2017;65(5):442–454. doi:10.1248/cpb.c16-00761
17. Gueiffier A, Mavel S, Lhassani M, et al. Synthesis of imidazo[1,2-*a*] pyridines as antiviral agents. *J Med Chem*. 1998;41(25):5108–5112. doi:10.1021/jm981051y
18. Helal MH, El-Awdan SA, Salem MA, et al. Synthesis, biological evaluation and molecular modeling of novel series of pyridine derivatives as anticancer, anti-inflammatory and analgesic agents. *Spectrochim Acta A Mol Biomol Spectrosc*. 2015;135:764–773. doi:10.1016/j.saa.2014.06.145
19. Mojarrab M, Soltani R, Aliabadi A. Pyridine based chalcones: synthesis and evaluation of antioxidant activity of 1-phenyl-3-(pyridin-2-yl)prop-2-en-1-one derivatives. *Jundishapur J Nat Pharm Prod*. 2013;8(3):125–130. doi:10.5812/jjnpp.
20. Yee CK, Ulman A, Ruiz JD, Parikh A, White H, Rafailovich M. Alkyl selenide- and alkyl thiolate-functionalized gold nanoparticles: chain packing and bond nature. *Langmuir*. 2003;19(22):9450–9458. doi:10.1021/la020628i
21. Jana NR, Pal T. Redox catalytic property of still-growing and final palladium particles: acomparative study. *Langmuir*. 1999;15 (10):3458–3463. doi:10.1021/la981512i
22. Kamat PV. Photochemistry on nonreactive and reactive (semiconductor) surfaces. *Chem Rev*. 1993;93(1):267–300. doi:10.1021/cr00017a013
23. Pradhan N, Pal A, Pal T. Catalytic reduction of aromatic nitro compounds by coinage metal nanoparticles. *Langmuir*. 2001;17 (5):1800–1802. doi:10.1021/la000862d
24. Kometani N, Tsubonishi M, Fujita T, Asami K, Yonezawa Y. Preparation and optical absorption spectra of dye-coated Au, Ag, and Au/Ag colloidal nanoparticles in aqueous solutions and in alternate assemblies. *Langmuir*. 2001;17(3):578–580. doi:10.1021/la0013190
25. Strimbu L, Liu J, Kaifer AE. Cyclodextrin-capped palladium nanoparticles as catalysts for the suzuki reaction. *Langmuir*. 2003;19 (2):483–485. doi:10.1021/la026550n
26. Liong M, Lu J, Kovochich M, et al. Multifunctional inorganic nanoparticles for imaging, targeting, and drug delivery. *ACS Nano*. 2008;2 (5):889–896. doi:10.1021/nn800072t
27. Brigger I, Dubernet C, Couvreur P. Nanoparticles in cancer therapy and diagnosis. *Adv Drug Deliv Rev*. 2002;54(5):631–651.
28. Das J, Han JW, Choi YJ, et al. Cationic lipid-nanoceria hybrids, a novel nonviral vector-mediated gene delivery into mammalian cells: investigation of the cellular uptake mechanism. *Sci Rep*. 2016;6:29197. doi:10.1038/srep29197
29. Sun Y, Xia Y. Shape-controlled synthesis of gold and silver nanoparticles. *Science*. 2002;298(5601):2176–2179. doi:10.1126/science.1077229
30. Baughman RH, Zakhidov AA, de Heer WA. Carbon nanotubes–the route toward applications. *Science*. 2002;297(5582):787–792. doi:10.1126/science.1060928
31. Sangomla S, Saifi MA, Khurana A, Godugu C. Nanoceria ameliorates doxorubicin induced cardiotoxicity: possible mitigation via reduction of oxidative stress and inflammation. *J Trace Elem Med Biol*. 2018;47:53–62. doi:10.1016/j.jtemb.2018.01.016
32. Saifi MA, Sangomla S, Khurana A, Godugu C. Protective effect of Nanoceria on cisplatin-induced nephrotoxicity by amelioration of oxidative stress and pro-inflammatory mechanisms. *Biol Trace Elem Res*. 2019;189(1):145–156. doi:10.1007/s12011-018-1457-0
33. Kumari P, Saifi MA, Khurana A, Godugu C. Cardioprotective effects of nanoceria in a murine model of cardiac remodeling. *J Trace Elem Med Biol*. 2018;50:198–208. doi:10.1016/j.jtemb.2018.07.011
34. Khurana A, Tekula S, Saifi MA, Venkatesh P, Godugu C. Therapeutic applications of selenium nanoparticles. *Biomed Pharmacother*. 2019;111:802–812. doi:10.1016/j.biopha.2018.12.146
35. Kamal T, Ul-Islam M, Khan SB, Asiri AM. Adsorption and photocatalyst assisted dye removal and bactericidal performance of ZnO/chitosan coating layer. *Int J Biol Macromol*. 2015;81:584–590. doi:10.1016/j.ijbiomac.2015.08.060
36. Khan SB, Ali F, Kamal T, Anwar Y, Asiri AM. CuO embedded chitosan spheres as antibacterial adsorbent for dyes. *Int J Biol Macromol*. 2016;88:113–119. doi:10.1016/j.ijbiomac.2016.03.026

37. Khan SA, Khan SB, Kamal T, Asiri AM, Akhtar K. Recent development of chitosan nanocomposites for environmental applications. *Recent Pat Nanotechnol*. 2016;10(3):181–188. doi:10.2174/1872210510666160429145339
38. Ahmed MS, Kamal T, Khan SA, et al. Assessment of anti-bacterial Ni-Al/chitosan composite spheres for adsorption assisted photo-degradation of organic pollutants. *Curr Nanosci*. 2016;12(5):569–575. doi:10.2174/1573413712666160204000517
39. Kavitha T, Haider S, Kamal T, Ul-Islam M. Thermal decomposition of metal complex precursor as route to the synthesis of Co_3O_4 nanoparticles: antibacterial activity and mechanism. *J Alloy Compd*. 2017;704:296–302. doi:10.1016/j.jallcom.2017.01.306
40. Kamal T, Ali N, Naseem AA, Khan SB, Asiri AM. Polymer nanocomposite membranes for antifouling nanofiltration. *Recent Pat Nanotechnol*. 2016;10(3):189–201. doi:10.2174/1872210510666160429145704
41. Haider A, Haider S, Kang I-K, et al. A novel use of cellulose based filter paper containing silver nanoparticles for its potential application as wound dressing agent. *Int J Biol Macromol*. 2018;108:455–461. doi:10.1016/j.ijbiomac.2017.12.022
42. Pervaiz M, Ahmad I, Yousaf M, et al. Synthesis, spectral and antimicrobial studies of amino acid derivative Schiff base metal (Co, Mn, Cu, and Cd) complexes. *Spectrochim Acta A Mol Biomol Spectrosc*. 2019;206:642–649. doi:10.1016/j.saa.2018.05.057
43. Abdallah AEM, Elgemeie GH. Design, docking, synthesis and antimicrobial evaluation of some novel pyrazolo[1,5-*a*]pyrimidines and their corresponding cycloalkane ring-fused derivatives as purine analogues. *Drug Des Devel Ther*. 2018;12:1785–1798. doi:10.2147/DDDT.S159310
44. Abdallah AEM, Mohareb RM, Khalil EM, Elshamy MAMA. Synthesis of novel heterocyclic compounds incorporate 4,5,6,7-tetrahydrobenzo[*b*]thiophene together with their cytotoxic evaluations. *Chem Pharm Bull*. 2017;65:469–477. doi:10.1248/cpb.c16-00925
45. Abdallah AEM, Helal MHE, Elakabawy NII. Heterocyclization, dyeing applications and anticancer evaluations of benzimidazole derivatives: novel synthesis of thiophene, triazole and pyrimidine derivatives. *Egypt J Chem*. 2015;58:699–719. doi:10.21608/EJCHEM.2015.1015
46. Abdallah AEM, Mohareb RM. Uses of 4,4-dicyano-3-phenyl-but-3-enoic acid phenylamide for the synthesis of new compounds: antimicrobial and textile finishing evaluations. *Pigm Res Tech*. 2019;48(2):89–107. doi:10.1108/PRT-11-2017-0085
47. Mohareb RM, Mahmoud AE, Abdelaziz MA. New approaches for the synthesis of pyrazole, thiophene, thieno[2,3-*b*]pyridine, and thiazole derivatives together with their anti-tumor evaluations. *Med Chem Res*. 2014;23:564–579. doi:10.1007/s00044-013-0664-7
48. Mohareb RM, Abdallah AEM, Mohamed AA. Synthesis of novel thiophene, thiazole and coumarin derivatives based on benzimidazole nucleus and their cytotoxicity and toxicity evaluations. *Chem Pharm Bull*. 2018;66(3):309–318. doi:10.1248/cpb.c17-00922
49. Helal MH. Synthesis and characterization of a new series of pyridinone azo dyes for dyeing of synthetic fibers. *Pigm Res Tech*. 2004;33(3):165–171. doi:10.1108/03699420410537287
50. Dwivedi C, Shah CP, Singh K, Kumar M, Bajaj PN. An organic acid-induced synthesis and characterization of selenium nanoparticles. *J Nanotechnol*. 2011;2011:651971. doi:10.1155/2011/651971
51. Trotman ER. *Dyeing and Chemical Technology of Textile Fibers*. 6th ed. London, UK/ Melbourne, Australia/Auckland,NZ: John Wiley & Sons Inc; 1984:306–309.
52. Society of Dyer and Colourists. *Standard Methods for the Determination of the Colour Fastness of Textiles and Leather*. 4th ed. Bradford, England (UK): The England Society; 1978.
53. RY WU. Studies on the Streptomyces SC4. II, Taxonomical and biological characteristics of *Streptomyces* strain SC4. *Bot Bull Acad Sin*. 1984;25:111–123.
54. Cooper KE. The theory of antibiotic inhibition zones. In: *Analytical Microbiology*. Kavanagh FBTAM, editor. London: Academic Press: New York; 1963:1–86.

International Journal of Nanomedicine Dovepress

Publish your work in this journal

The International Journal of Nanomedicine is an international, peer-reviewed journal focusing on the application of nanotechnology in diagnostics, therapeutics, and drug delivery systems throughout the biomedical field. This journal is indexed on PubMed Central, MedLine, CAS, SciSearch®, Current Contents®/Clinical Medicine, Journal Citation Reports/Science Edition, EMBase, Scopus and the Elsevier Bibliographic databases. The manuscript management system is completely online and includes a very quick and fair peer-review system, which is all easy to use. Visit http://www.dovepress.com/testimonials.php to read real quotes from published authors.

Submit your manuscript here: https://www.dovepress.com/international-journal-of-nanomedicine-journal